

# Piezoelectric Potential Output from ZnO Nanowire Functionalized with p-Type Oligomer

Jinhui Song,<sup>†</sup> Xudong Wang,<sup>†</sup> Jin Liu,<sup>†</sup> Huibiao Liu,<sup>†,‡</sup> Yuliang Li,<sup>‡</sup> and Zhong Lin Wang<sup>\*,†</sup>

*School of Materials Science and Engineering, Georgia Institute of Technology, Atlanta, Georgia 30332-0245, and CAS Key Laboratory of Organic Solid, Beijing National Laboratory for Molecular Sciences (BNLMS), Institute of Chemistry, Chinese Academy of Sciences, Beijing 100080, People's Republic of China*

Received September 21, 2007; Revised Manuscript Received November 28, 2007

## ABSTRACT

We have studied the piezoelectric potential output of a ZnO wire/belt functionalized with p-type oligomer (2,5-Bis(octanoxy)-1,4-bis(4-formyl phenylene vinylene) benzene) (OPV2) when it was deflected by an atomic force microscope (AFM) tip in contact mode. In comparison to the ZnO wire/belt without oligomer coating, an extra positive voltage peak was observed prior to the appearance of a negative potential peak. The paired positive and negative voltage peaks are the results of tip contact to the stretched and the compressed side of the wire/belt, corresponding to the positive and negative local piezoelectric potential, respectively. The p–n junction between OPV2 and ZnO serves as a “diode” that controls the flow of current. When the nanowire/nanobelt is first bent by the AFM tip, the diode is reversely biased and the piezoelectric charges are stored in the ZnO wire/belt. As the AFM tip further bends the wire/belt, the local piezoelectric potential is continuously accumulated to a value that is large enough to break through the diode. Then the free charges from the external circuit can flow in and neutralize/screen part of the piezoelectric charges, resulting in a positive pulse in the output signal. When the AFM tip continues to scan to reach the compressed side of the ZnO wire/belt, the p–n junction is forwardly biased. Neutralizing/screening the residual and the newly created piezoelectric charges leads to the flow of current from the tip to the ZnO wire/belt, resulting in a negative voltage pulse. This study supports the charging and discharging model proposed for the piezoelectric nanogenerator.

ZnO is a smart material that is widely used in semiconductor industry, and it is a very attractive material for studying nanoscale phenomena. Recently, we have used nanowire (NW) arrays of ZnO for converting mechanical energy into electricity.<sup>1,2</sup> The principle of the nanogenerator relies on the coupled semiconducting and piezoelectric properties.<sup>3,4</sup> When a clean ZnO nanowire or nanobelt is bent by an atomic force microscope (AFM) tip as a result of piezoelectricity, the stretched side of the NW has a positive potential and its compressed side has a negative potential in reference to the grounded bottom end. Because of the existence of a Schottky barrier between the AFM metal tip and the ZnO NW, the contact between the tip and the stretched side is a reversely biased Schottky diode, while the contact with the compressed side is a forward-biased Schottky diode; a charge creation-accumulation and charge release process is created at the interface when the tip scans across the NW, resulting in a current flowing from the metal tip to the ZnO NW. The voltage drop across an external load shows a negative voltage

pulse. This is the process of the piezoelectric energy conversion.

It is well known that the surface chemical and physical properties of a semiconductor oxide can be substantially improved by polymer functionalization.<sup>5</sup> As a unique advantage of NWs, surface functionalization can drastically improve its performances, such as its UV response and conductivity.<sup>6,7</sup> The mechanism of the nanogenerator largely depends on the surface contact, which may critically affect the charge accumulation and release process. Surface functionalization is therefore expected to be an effective pathway to alternate, rectify, or enhance the potential output. In this paper, we report the investigation about the piezoelectric output of a ZnO wire/belt coated with a thin layer of p-type oligomer. An explanation is provided about the observed “abnormal” output voltage, which provides additional evidence about the mechanism proposed previously for the piezoelectric nanogenerator.

Our experiment was based on mechanical manipulation of a single ZnO wire/belt using AFM.<sup>3</sup> The selected ZnO wire/belt was long enough to be directly visualized under optical microscope built in AFM. One end of the ZnO wire/

\* To whom correspondence should be addressed. E-mail: zhong.wang@mse.gatech.edu.

<sup>†</sup> Georgia Institute of Technology.

<sup>‡</sup> Chinese Academy of Sciences.

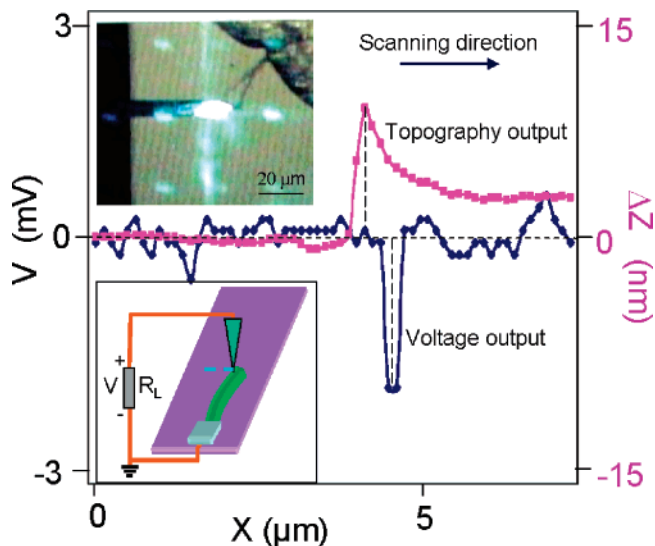


**Figure 1.** In situ observation of the process of outputting piezoelectric potential by scanning an one-end-free ZnO wire/belt using an AFM tip. The ZnO is clean without oligomer coating. Top inset is a snapshot optical image of the AFM tip that is deflecting the wire/belt. Bottom inset is a schematic experimental setup. The curves are the aligned plot of the output voltage (blue curve) over the external load and the topography profile (pink curve).

belt was fixed on to a flat intrinsic silicon substrate using silver paste that is electrically grounded; the other end was left free (see the lower left corner inset in Figure 1). The silicon substrate was an insulator. The ZnO wire/belt was laid parallel to and a little bit above the substrate in free suspension to eliminate friction. A resistor  $R_L = 500 \text{ M}\Omega$  is connected between the fixed end of the ZnO wire/belt and the AFM tip, and the output signal is characterized by a voltage drop across the resistor in reference to the grounded end. The measurement was performed using an AFM (model MFP-3D from Asylum research) with a Pt-coated silicon tip (Electri-Lever AC240 from Asylum research), which has a tetrahedral tip of  $14 \mu\text{m}$  in height. The cantilever has a spring constant of  $1.6 \text{ N/m}$ . All of the measurements were performed in contact mode with a set point of  $5 \text{ nN}$  and a scanning speed between  $60$  and  $160 \mu\text{m/s}$ . No external voltage was applied at any stage of the experiment. Both the topography and potential output ( $V$ ) images on the resistor were monitored simultaneously during the tip scanning. The entire experiment was recorded at video rate so that the electric energy generation process can be directly visualized. The data presented in the figures were snapshots of the characteristic events extracted from the video and the corresponding experimental data.

For comparison purpose, we first studied the piezoelectric output from a clean ZnO wire/belt that had no surface coating. During the scan, when the tip only touched the stretched side of the wire/belt and did not lift up to go beyond the central line of the wire/belt to reach the compressed side, there was no voltage output signal. The output voltage peak was observed only when the tip went beyond the wire/belt to reach its compressed side, as characterized by a peak in the topography image (pink curve) in Figure 1. The corre-

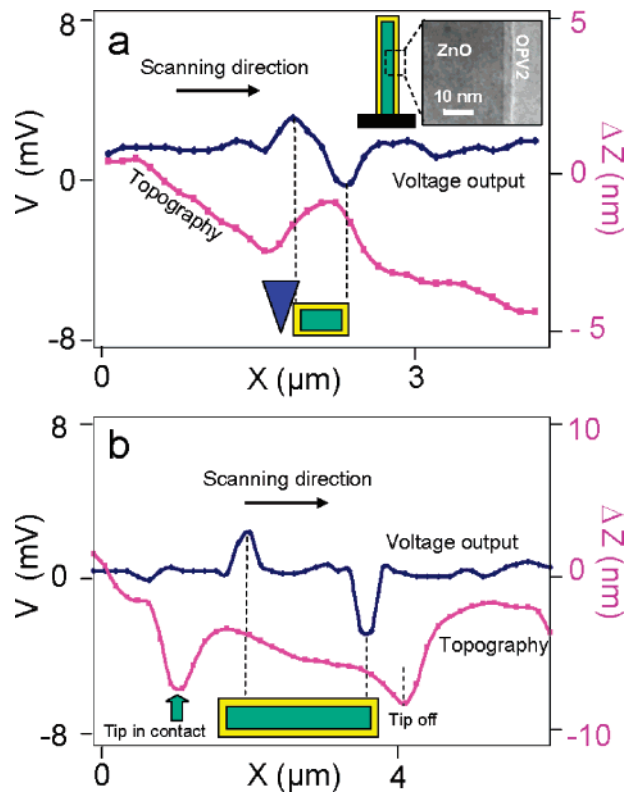


**Figure 2.** In situ observation of the process of outputting piezoelectric potential of a one-end-free ZnO wire/belt that is coated with a thin layer of OPV2. (a,b) Aligned plot of the output voltage (blue curve) over the external load and the topography profile (pink curve) measured from two different wires/belts. Top inset is a TEM image showing the thickness of the oligomer coating. Schematic cross-section of the wire/belt is illustrated.

sponding output voltage is represented by the blue curve in Figure 1, which is always a negative peak in reference to the grounded end of the wire/belt. It is also important to note that the center of the voltage peak was delayed in reference to the peak in the topography image. These are the most important characteristics for a ZnO wire/belt without surface functionalization, and they have been explained as a result of a “switch effect” created by the Schottky barrier between the AFM tip and the ZnO wire/belt.<sup>1,3</sup>

We now present the case when the ZnO wire/belt was coated with a thin layer of OPV (oligomer (*p*-phenylene vinylene)) derivatives,<sup>8</sup> which were selected because they are extensively studied *p*-type oligomers for light-emitting, field-effect transistors, and supramolecular assembly and are amphiphilic due to their high absorption coefficient, strong donating ability, and good thermal, chemical, and photochemical stability.<sup>9,10,11,12</sup> The as-synthesized ZnO wire/belt was immersed in 1% Mol/L (alpha,omega-bis(methylthioacetate) oligo(phenylene vinylene)-COOH) (OPV2) menthol solution for 48 h. Then, the wire/belt was taken out and rinsed by deionized water and dried in air. A 2–3 nm thick OPV2 was coated on the surface of the ZnO wire/belt (see the inset transmission electron microscopy (TEM) image in Figure 2). Using this functionalized wire/belt, we performed the same experiment as described in Figure 1, and a typical voltage output is presented in Figure 2a. In contrast to the

case of the ZnO wire/belt without surface functionalization, a pair of positive and negative output voltage peaks were observed. The positive peak appeared when the tip was in contact with the stretched side of the wire/belt, and the negative peaks showed up when the tip was in contact with the compressed side, which was determined by examining the peak positions in reference to the signal in the topography image. The uneven background in the topography image is caused by the downward bending and/or slight vibration of the free-standing wire/belt during the scan. In our experiments, some of the scans produced only positive voltage pulses, some generated only negative pulses, and some generated both. In reference to the information provided by the topography image, the negative pulse was generated only when the AFM tip scanned over the central line and reached the compressed side of the wire/belt, which is consistent to our previous observation.<sup>1,3</sup>

Figure 2b shows a typical tip scan profile across a ZnO belt, in which both the positive and negative pulses were generated when the tip scanned from the stretched side to the compressed side of the belt. In the contact mode, the tip was lifted up by the belt to keep a constant normal force. Because the belt was freely suspended, it may move slightly downward or even vibrate when it was pushed by the tip, thus, the uneven background was recorded. Moreover, the width of the topography profile was rather wide in comparison to the actual width of the wire/belt because the wire/belt was continuously pushed and bent when the image was acquired. The vertical distance,  $\Delta Z$ , may not be the actual thickness of the wire/belt owing to its free-standing configuration and the shape of the tip. The positions at which the tip touched the belt and started to lift up can be clearly identified, as indicated by an arrowhead in Figure 2b. By correlating the relative position of the voltage peak to the topography image of the belt, no voltage was released when the tip first contacted the belt. The positive voltage peak appeared after the tip pushed the belt for  $\sim 0.5 \mu\text{m}$  along the scanning direction. This indicates that the belt had to be bent to a certain angle/distance before the voltage pulse was released. The delayed discharging peak clearly shows that a simple physical contact cannot produce the voltage pulse, which rules out the contributions from surface/volume electrostatic charge, friction charge, or even measurement circuit. As for the negative voltage peak, it appeared that the voltage pulse was released before the tip lost contact with the belt, as indicated by the dip in the topography curve.

To understand the phenomena we observed in Figure 2, the transport properties of the ZnO wire/belt, OPV2, and OPV2-functionalized ZnO wires were characterized. Two pieces of ZnO NW arrays were cut from the same sample grown on indium tin oxide (ITO) glass substrate with only one of them being functionalized with OPV2. To maintain the reliability and stability of the  $I$ - $V$  measurements, two  $\sim 2 \text{ mm}^2$  size Pt electrodes were employed for the contact measurements. One Pt electrode was connected to the bottom ITO layer, and the other Pt electrode was put in contact to the tips of the nanowire arrays, as shown in the inset of Figure 3. The externally applied voltage was swapped from

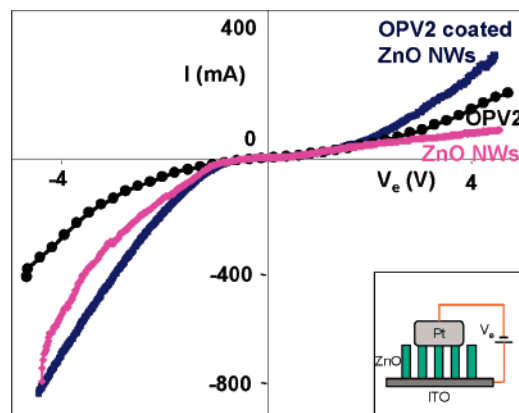


**Figure 3.**  $I$ - $V$  characteristics of the contacts between Pt electrode and ZnO nanowires without coating (pink), Pt electrode and OPV2 (black), and Pt electrode and OPV2-functionalized ZnO nanowires (blue). Inset is a schematic diagram of the experiment set up. A flat Pt electrode was placed on the top of the aligned ZnO nanowire with or without coating a layer of p-type oligomer.

$-5$  to  $5 \text{ V}$ . The  $I$ - $V$  curve shows that the contact between Pt and ZnO nanowire is a typical Schottky contact (pink curve in Figure 3). To characterize the contact between Pt electrode and OPV2, an  $I$ - $V$  measurement was performed on an OPV2-covered ITO glass substrate, where one electrode contacted ITO glass and the other one was in contact with the OPV2 layer. The contact between Pt and OPV2 is ohmic (black curve in Figure 3). The contact between OPV2-coated ZnO NWs and the Pt electrode is a nonsymmetric curve. When  $0 < V_e < 1.5 \text{ V}$ , the  $I$ - $V$  characteristic is the Schottky type, but when  $V_e > 1.5 \text{ V}$ , the  $I$ - $V$  curve starts to show the ohmic behavior. This indicates that the p-n junction can be broken through when the local potential is larger than  $\sim 1.5 \text{ V}$ . For a large belt used in our experiments of a few hundred nanometers in width, the local piezoelectric potential can be a few to a few tens of volts according to the calculation (eq 1).<sup>13</sup> Thus, it is possible to have a local break through at large deflections. It is apparent that the OPV2 coating has changed the transport properties of the contacts, which is important for understanding the phenomenon presented in Figure 2.

After knowing the contact characteristics, we proposed a model for understanding the voltage signals shown in Figure 2. Our model is based on the mechanism presented previously for understanding the charge creation-accumulation and charge-releasing processes proposed for a clean ZnO wire/belt.<sup>1,3</sup> By bending a ZnO wire/belt, an asymmetric strain distribution across its width results in an asymmetric potential distribution with a positive potential ( $V_s^+ > 0$ ) at its stretched side and negative potential ( $V_s^- < 0$ ) at the compressed side in reference to the grounded-fixed-end.<sup>13</sup> Typically, an as-grown ZnO NW is n-type. For a clean ZnO wire/belt without oligomer coating, a Schottky diode is presented at the interface between the Pt tip and the n-type ZnO wire/belt, which controls the charge accumulating and releasing process. Because the work function of Pt is  $6.1 \text{ eV}$ , and the electron affinity of ZnO is  $4.5 \text{ eV}$ ,<sup>14</sup> the Pt-ZnO contact is Schottky with a barrier height of  $1.6 \text{ eV}$  for bulk materials. Recent scanning tunneling microscopy



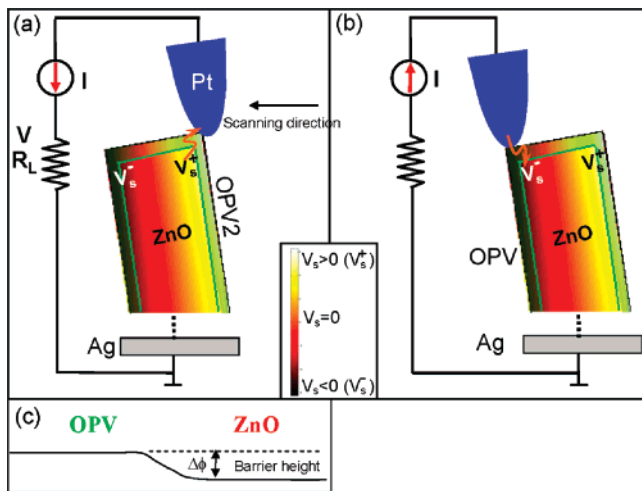


**Figure 4.** Proposed model of the piezoelectric potential generated from an OPV2-coated ZnO wire/belt when deflected by an AFM tip. (a,b) Metal and semiconductor contacts between the AFM tip and the semiconductor ZnO belt coated with OPV2 at positive and negative local contact potential (see text). (c) Schematic diagram showing the barrier height at the OPV2–ZnO p–n junction.

experimental measurement shows that the barrier for nanocontact is 0.45 eV and is very sensitive to local strain, which is significantly lower than that of bulk contact.<sup>15</sup> The piezoelectric potential  $V_s^+$  is proportional to the degree of bending of the wire/belt, and it is simply described by a simple formula<sup>13</sup> of

$$V_s^\pm \approx \pm 27 (a/L)^3 y_m \quad (\text{in V}) \quad (1)$$

where  $a$  and  $L$  are the radius and length of the NW, respectively, and  $y_m$  (in nm) is the lateral displacement at tip of the NW. For a typical wire of  $a = 1 \mu\text{m}$ ,  $L = 40 \mu\text{m}$ , and  $y_m = 10 \mu\text{m}$  (see Figure 1), the maximum potential at the surface is  $(V_s^\pm)_{\text{max}} \approx \pm 4.2 \text{ V}$ .

When the ZnO wire/belt is functionalized with a thin layer of OPV2, the Pt tip is separated from the n-type ZnO wire/belt by this p-type oligomer. Because the contact between Pt and ZnO is ohmic, the carrier transportation from Pt to ZnO is controlled by the p–n junction formed between OPV2 and ZnO. From the  $I$ – $V$  characteristic presented in Figure 3, it is likely that the p–n junction barrier height  $\Delta\phi$  between OPV2 and ZnO is lower than Schottky barrier height between Pt and ZnO. When the tip first touches the OPV2 coated wire/belt (Figure 4a), it deflects the wire/belt and the piezoelectric charges are continuously produced, but the local potential  $V_s^+$  created is smaller than the barrier height because  $V_s^+$  is proportional to the lateral deflection of the nanowire (eq 1). Thus, the p–n junction at the OPV2–ZnO interface is reversely biased (Schottky type). In this case, the charges are accumulated without releasing due to the rectifying effect of the p–n junction. With the further increase of bending, the local piezoelectric potential  $V_s^+$  becomes larger than the barrier height  $\Delta\phi$  (Figure 4c) and the p–n junction is broken through (ohmic type). Thus, the current flows from the ZnO wire/belt into Pt tip through the OPV2 layer resulting in the positive potential peaks as presented in Figure 2.

If the Pt tip scans fast across the wire/belt, two possible consequences could result. First, the contacting time may be so short that the piezoelectric charges could not be completely neutralized/screened by the external electrons if the carrier density and carrier mobility were low in OPV2. As a result, a small potential may still be preserved even after neutralizing/screening part of the charges. The other possibility is that the wire/belt could be continuously bent when the tip scanned from the stretched side to the compressed side, which generates additional potential with the increase of deformation. When the conductive tip reaches the compressed side of the ZnO wire/belt, the negative piezoelectric potential  $V_s^-$  at the ZnO side sets the p–n junction to forward bias, resulting in a flow of current from the Pt tip into the ZnO wire/belt, thus negative voltage pulses are observed (Figure 2). In an alternative case, if all of the charges are neutralized/screened when the tip contacts the stretched side of the wire and no more deflection is introduced when the tip slides to the compressed side, there will be no negative pulse output. This is likely the reason that only a positive pulse is observed in some of the scans.

The conductivity of the OPV is important for the observation of the reported phenomenon. If its conductivity is too high, the created piezoelectric potential in the NW may be quickly screened by the charges in OPV within a time period shorter than the contacting time of the scanning tip with the NW. If its conductivity is too low, the flow of current through OPV is rather limited, possibly resulting in very low output voltage. An optimum choice of conductivity is important.

In summary, we have investigated the piezoelectric potential output of a ZnO wire/belt functionalized with p-type oligomer OPV2 when it was deflected by an AFM tip in contact mode. Paired positive and negative voltage peaks were observed when the tip scanned from the stretched side to the compressed side of the wire/belt, which is explained as a result of outputting the local positive and negative piezoelectric potential as “gated” by a p–n junction between OPV2 and n-type ZnO wire/belt. This study supports the charging and discharging model proposed for the piezoelectric nanogenerator.

**Acknowledgment.** This work was supported by DOE BES (DE-FG02-07ER46394), NSF (DMS 0706436), and the Major State Basic Research development Program (2006CB-932100). Thanks to Sheng Xu, Yifan Gao, and Wenjie Mai for discussion.

## References

- (1) Wang, Z. L.; Song, J. H. *Science* **2006**, *312*, 242.
- (2) Wang, X. D.; Song, J. H.; Liu, J.; Wang, Z. L. *Science* **2007**, *316*, 102.
- (3) Song, J. H.; Zhou, J.; Wang, Z. L. *Nano Lett.* **2006**, *6*, 1656–1662.
- (4) Wang, X. D.; Liu, J.; Song, J. H.; Wang, Z. L. *Nano Lett.* **2007**, *7*, 2475.
- (5) Li, Y.; Wong, C. P. *Appl. Phys. Lett.* **2006**, *89*, 112112.
- (6) Lao, C. S.; Li, Y.; Wong, C. P.; Wang, Z. L. *Nano Lett.* **2007**, *7*, 1323.
- (7) Lao, C. S.; Park, P. C.; Kuang, Q.; Deng, Y. L.; Sood, A. K.; Polla, D. L.; Wang, Z. L. *J. Am. Chem. Soc.*, in press.
- (8) Praveen, V. K.; George, S. J.; Varghese, R.; Vijayakumar, C.; Ajayaghosh, A. *J. Am. Chem. Soc.* **2006**, *128*, 7542.

- (9) Liu, T.; Li, Y.; Gan, H.; Li, Y.; Liu, H.; Wang, S.; Zhou, W.; Wang, C.; Li, X.; Liu, X.; Zhu, D. *Tetrahedron* **2007**, *63*, 232.
- (10) (a) Nagata, T.; Osuka, A.; Maruyama, K. *J. Am. Chem. Soc.* **1990**, *112*, 3054. (b) Gaylord, B. S.; Wang, S.; Heeger, A. J.; Bazan, G. C. *J. Am. Chem. Soc.* **2001**, *123*, 6417.
- (11) George, S. J.; Ajayaghosh, A.; Jonkheijm, P.; Schenning, A. P. H. J.; Meijer, E. W. *Angew. Chem., Int. Ed.* **2004**, *43*, 3422.
- (12) (a) Jonkheijm, P.; Hoeben, F. J. M.; Kleppinger, R.; van Herikhuyzen, J.; Schenning, A. P. H. J.; Meijer, E. W. *J. Am. Chem. Soc.* **2003**, *125*, 15941. (b) Wolfs, M.; Hoeben, F. J. M.; Beckers, E. H. A.; Schenning, A. P. H. J.; Meijer, E. W. *J. Am. Chem. Soc.* **2005**, *127*, 13484.
- (13) Gao, Y. F.; Wang, Z. L. *Nano Lett.* **2007**, *7*, 2499.
- (14) Hasegawa, S.; Nishida, S.; Yamashita, T.; Asahi, H. *J. Ceramic Process. Res.* **2005**, *6*, 245.
- (15) Perez-Garcia, B.; Zuñiga-Perez, J.; Munoz-Sanjose, V.; Colchero, J.; Palacios-Lidon, E. *Nano Lett.* **2007**, *7*, 1505.

NL072440V